

Research on Forecasting Framework for System Marginal Price based on Deep Recurrent Neural Networks and Statistical Analysis Models

Taehyun Kim^{§,1}, Yoonjae Lee^{§,1}, and Soonho Hwangbo^{1,2,*}

¹Department of Chemical Engineering, Gyeongsang National University,
Jinju-si, 52828, Korea

²Department of Materials Engineering and Convergence Technology, Gyeongsang National University,
Jinju-si, 52828, Korea

(Received for review April 11, 2022; Revision received May 17, 2022; Accepted May 20, 2022)

Abstract

Electricity has become a factor that dramatically affects the market economy. The day-ahead system marginal price determines electricity prices, and system marginal price forecasting is critical in maintaining energy management systems. There have been several studies using mathematics and machine learning models to forecast the system marginal price, but few studies have been conducted to develop, compare, and analyze various machine learning and deep learning models based on a data-driven framework. Therefore, in this study, different machine learning algorithms (i.e., autoregressive-based models such as the autoregressive integrated moving average model) and deep learning networks (i.e., recurrent neural network-based models such as the long short-term memory and gated recurrent unit model) are considered and integrated evaluation metrics including a forecasting test and information criteria are proposed to discern the optimal forecasting model. A case study of South Korea using long-term time-series system marginal price data from 2016 to 2021 was applied to the developed framework. The results of the study indicate that the autoregressive integrated moving average model (R-squared score: 0.97) and the gated recurrent unit model (R-squared score: 0.94) are appropriate for system marginal price forecasting. This study is expected to contribute significantly to energy management systems and the suggested framework can be explicitly applied for renewable energy networks.

Keywords: Electricity price forecasting, Machine learning, Deep learning, Optimal model selection, Energy management systems

1. Introduction

From the perspective of supply and demand in the electricity market, there are a variety of inevitable factors that affect both demand and supply (e.g., soaring demand, energy policy, and raw material price) [1, 2]. In the case of the traditional power trading market, it generally consists of exchanges, power plants, and consumers [3]. For instance, the retail electricity portion in South Korea relies on the Korea Electric Power Corporation and the South Korean electricity price depends on six power generation companies (e.g., Korea Hydro & Nuclear Power, Korea South-East Power, Korea Midland Power, Korea Western Power, Korea Southern Power, and Korea East-West Power). The Korean electric power market has the following three characteristics [4]: 1) there exists

a mandatory power pool except for small-scale renewables less than 1 MW with private LNG power generators or unconnected islands that trade directly with Korea Electric Power Corporation; 2) cost-based pool (CBP) market (i.e., the power generation fluctuation ratio is determined in advance according to power generators' bid); and 3) a day-ahead market, in which the transaction price is determined one day earlier. The day-ahead market is explicitly related to the system marginal price (SMP), which is underpinned by the variable ratio of marginal generators to the market price while making sure to meet the forecast demand for each hour [5]. The SMP is associated with the result from the combination of different dispatchable power generators, which implies that it is equal to the most expensive electricity generation price among all available power generators [6].

[§]The first and second author contributed equally in this research.

* To whom correspondence should be addressed.

E-mail: s.hwangbo@gnu.ac.kr; Tel: +82-55-772-1784; Fax: +82-55-772-1789

doi: 10.7464/kscet.2022.28.2.138 pISSN 1598-9712 eISSN 2288-0690

This is an Open-Access article distributed under the terms of the Creative Commons Attribution Non-Commercial License (<http://creativecommons.org/licenses/by-nc/3.0>) which permits unrestricted non-commercial use, distribution, and reproduction in any medium, provided the original work is properly cited.

Table 1. Primary factors for the SMP

Factor	Description	Reference
Oil price	Great fluctuations in problems of high electricity demand, transportation, and delivery.	[8, 9]
Plant cost	Financing, construction, maintenance, and operating costs.	[10, 11]
Distribution	Connection between power plants and consumers.	[11, 12]
Weather	Increase in demand for heating or cooling.	[13–15]
Regulation	In some regions, public service/utility committees completely regulate prices.	[16, 17]

Therefore, it is of great importance to accurately predict SMP prices to contribute to energy management systems. Although the main factors that affect the SMP are well known, developing forecasting models for the SMP can present a challenge because they contain a number of underlying variables [18].

Accordingly, studies on SMP forecasting have been consistently conducted [19]. The generalized autoregressive conditional heteroscedasticity model was developed to estimate SMP volatility and examine the effect of power supply on the SMP [20]. Detailed information regarding SMP prediction from a mathematical model provided insight into the operating conditions of the Korean power market [21]. In addition, stochastic time-series, causal, and machine learning models to predict the SMP have been suggested and compared with one another through quantitative analysis [22]. Another comparative study to determine the performance between a mathematical model and a machine learning model for electricity rate prediction has also been presented [23].

Recently, research on deep learning-based forecasting models has attracted much attention. Deep learning uses a computational model consisting of hidden processing layers as a detailed field of machine learning that can be learned and predicted by discovering rules or structures among various and complex data [24]. For time-series data, the recurrent neural network (RNN) [25], long short-term memory (LSTM) [26], gated recurrent unit (GRU) [27], or bidirectional LSTM (BiLSTM) [28] can outperform other deep learning algorithms [29]. A hybrid LSTM model in combination with the wavelet transform has been proposed to improve prediction accuracy [30]. In another study, a hybrid model incorporating the wavelet transform, LSTM, and stacked auto-encoder was developed to enhance the existing forecasting model [31].

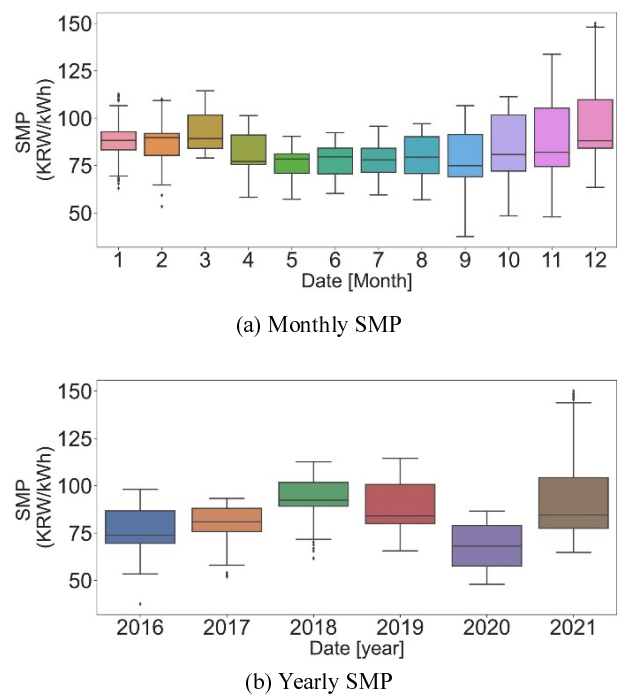
However, there have been few studies on the design of the framework for SMP forecasting, including data processing, model development, and model evaluation from the perspective of a data pipeline. The SMP depends on the price of various raw materials such as crude oil that is normally determined around 2 to 3 weeks earlier and also it is related to principles of energy demand/supply. Therefore, the proposed SMP forecasting model can contribute to the energy system management, particularly indicating that companies take advantage of it (i.e., in the case of South Korea, approximately 63% of the total energy demand is consumed in industries).

To this end, in this study, the following steps are implemented. First, long-term time-series data related to electricity are processed. Second, different forecasting models considering conventional machine learning and deep learning are developed. Third, a tuning technique that determines the optimal hyper-parameters is integrated. Fourth, results from the suggested models are demonstrated using various evaluation metrics. Lastly, the optimal forecasting models to be fit-for-purpose for a case study are selected via information criteria.

2. Material and methods

2.1 Data preparation

Figure 1 illustrates the general trend of the SMP for the last six years obtained from the Korea Power Exchange (KPX). The figure shows that the standard deviation of the SMP for the summer months (May to August) in South Korea is approximately 9.13, about half of that for the rest of the seasons, which is approximately 18.07. In addition, since October 2021, there has been a sharp


Figure 1. Time-series SMP data for South Korea.

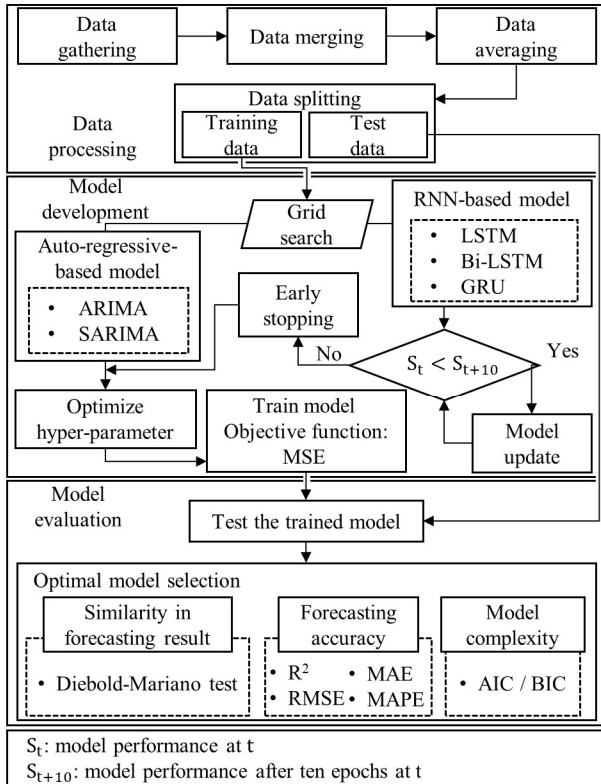


Figure 2. Framework of the SMP forecasting model.

rise in the SMP, an occurrence of which has not been observed before.

2.2 Algorithm for the framework of the SMP forecasting model

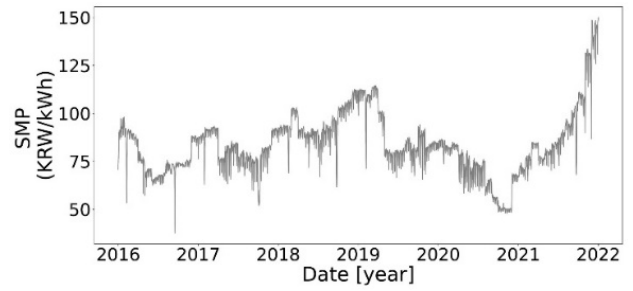
The aim of this study is to develop an optimal forecasting model of the SMP using an artificial intelligence-based framework to contribute to the improvement of the power system.

Figure 2 depicts the proposed framework of this study, which consists of data processing, model development, and model evaluation.

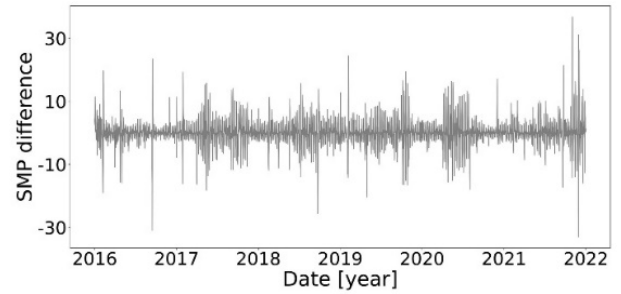
The main steps of the data processing include data collection, data averaging to improve model performance, and data splitting to prepare for supervised learning. According to the KPX, SMP data are estimated per hour; therefore all SMP datasets are converted into daily data by averaging them. In doing so, it is expected that overfitting is prevented and model performance is improved. Furthermore, inevitable outliers can be smoothed and harmonized with the rest of the data. Finally, processed time-series data are separated into input and output to be fit-for-purpose for supervised learning.

2.2.1 Machine learning-based forecasting model

The autoregressive integrated moving average (ARIMA), which is a typical approach to machine learning for time-series forecasting



(a) SMP raw data trend



(b) Results of the differencing operation

Figure 3. Stationary data process using the differences between two consecutive days.

models, forecasts future events using p observations and q prediction errors after the conversion of stationary time-series data using a differencing operation (Eq. (1)) [32]. A model that applies seasonality in the ARIMA is called a seasonal autoregressive integrated moving average (SARIMA) model [33].

$$y_t = c + \varphi_1 y'_{t-1} + \dots + \varphi_p y'_{t-p} + \theta_1 \varepsilon_{t-1} + \theta_2 (1) \varepsilon_{t-2} + \dots + \theta_q \varepsilon_{t-q} \quad (1)$$

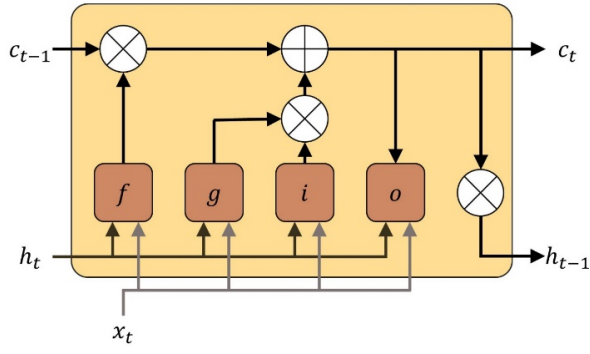
In stationary time-series data, the characteristics of the data do not change over time, and it is easy to analyze data with a constant mean and variance. When the mean and variance of the data are not constant, logarithmic-scale is taken to make data stationary; if the data show a trend or season, the data are converted into stationary data using a differencing operation [34], an approach of which is used in this study (Figure 3).

2.2.2 Deep learning-based forecasting model

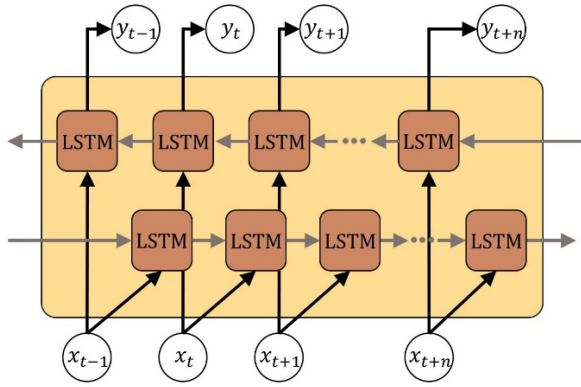
LSTM is a structure that learns by influencing the hidden layer through backpropagation (Figure 4(a)). Bidirectional LSTM (BiLSTM) is a modified LSTM that solves the problem related to the low learning ability of the initial cell in the LSTM (Figure 4(b)). The GRU is a specialized long-term memory model, which requires less demanding computing power than the LSTM (Figure 4(c)). The primary equations in the GRU network are as follows:

$$r_t = \text{sigm}(W_r[h_{t-1}, x_t]) \quad (2)$$

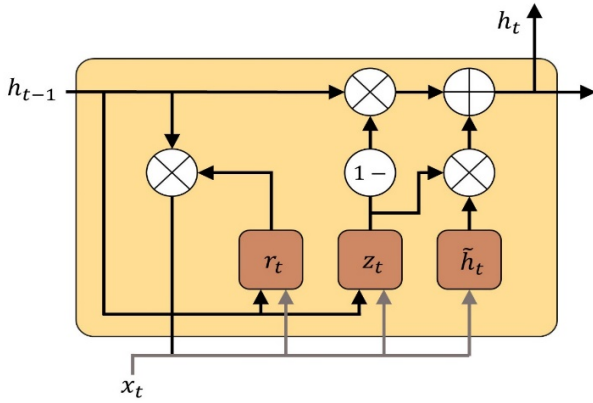
$$\tilde{h}_t = \text{tanh}(W_h[r_t \odot h_{t-1}, x_t]) \quad (3)$$



(a) Structure of the LSTM network



(b) Structure of the BiLSTM network



(c) Structure of the GRU network

Figure 4. Proposed deep learning-based forecasting models.

$$z_t = \text{sigm}(W_z[h_{t-1}, x_t]) \quad (4)$$

$$h_t = (1 - z_t) \odot h_{t-1} + z_t \odot \tilde{h}_t \quad (5)$$

where W_r is a matrix of weights for input data x_t and hidden unit h_{t-1} at reset gate r_t , W_h is a matrix of weights for x_t and h_{t-1} at temporarily hidden gate \tilde{h}_t , and W_z is a matrix of weights for x_t and h_{t-1} at update gate z_t . Each gate has biases. The reset gate selects how much past information to forget through the sigmoid function result of the weighted summation of the previous hidden state and the current input data (Eq. (2)). The temporarily hidden

gate is a prerequisite for obtaining the hidden gate dependent on the hyperbolic tangent (Eq. (3)). The update gate works for the previous hidden state and the temporarily hidden gate (Eqs. (4) and (5)).

In the case of the LSTM network, short-term memory must be considered.

$$f_t = \text{sigm}(W_{hf}h_{t-1} + W_{xf}x_t) \quad (6)$$

$$i_t = \text{sigm}(W_{hi}h_{t-1} + W_{xi}x_t) \quad (7)$$

$$g_t = \text{tanh}(W_{hg}h_{t-1} + W_{xg}x_t) \quad (8)$$

$$c_t = f_t \odot c_{t-1} + i_t \odot g_t \quad (9)$$

$$o_t = \text{sigm}(W_{ho}h_{t-1} + W_{xo}x_t) \quad (10)$$

$$h_t = o_t \odot \text{tanh}(c_t) \quad (11)$$

where W_{hf} , W_{hi} , W_{hg} , and W_{ho} are matrices of weights associated with the hidden state h_{t-1} of each gate, and W_{xf} , W_{xi} , W_{xg} , and W_{xo} are weights associated with input data x_t . The forget gate f_t that relies on the previous hidden state h_{t-1} and the input data determines whether or not information remains using the sigmoid function (Eq. (6)). The input gate i_t is similar to the forget gate but has the objective to remember the current information (Eq. (7)). At the same time, the input modulation gate g_t depends on the previous hidden state, the input data, and hyperbolic tangent function (Eq. (8)). The update gate c_t is the result based on Eqs. (6-8) (Eq. (9)). The output gate o_t uses the previous hidden state and the current input data (Eq. (10)). The hidden state h_t is calculated by the update gate and the output gate (Eq. (11)). In the BiLSTM, the major mathematical expressions are identical to those in the aforementioned LSTM network.

2.2.3 Hyper-parameter optimization using grid search

Grid search is a technique to determine the optimal hyper-parameters among all possible hyper-parameters [35]. The ARIMA or SARIMA sets the grid based on specific functions such as the autocorrelation function and partial autocorrelation function; otherwise, the grid search for deep learning models is implemented using the feasible range of hyper-parameters. The optimal hyper-parameters can be estimated considering the complexity and the performance score of the forecasting models. In this study, suggested models are run on an Intel Core i7-10700 CPU @2.90 GHz, 16.0 GB RAM, and NVIDIA GeForce GTX 1650 GPU.

Table 2. Optimal hyper-parameters for the machine learning and deep learning models.

Model	Hyper-parameter	Range	Optimal value
RNN based model (BiLSTM, LSTM, GRU)	Moving window	5, 7, 15, 30, 45, 60	7
	Number of nodes	10, 20, 40, 60, 100	40
	Batch size	10, 20, 40	10
ARIMA	p	0 to 20	8
	d	0 to 20	1
	q	0 to 20	1
SARIMA	p	0 to 20	8
	d	0 to 20	1
	q	0 to 20	1
	P	0 to 20	2
	D	0 to 20	0
	Q	0 to 20	2
	m	3, 6, 12, 24	12

Moving window: The number of previous data to predict day-ahead SMP, Node: Cell that calculates in an artificial neural network, p: Trend autoregression order; d: Trend difference order; q: Trend moving average order; P: Seasonal autoregressive order; D: Seasonal difference order; Q: Seasonal moving average order; m: Number of time steps for a single seasonal period

2.2.4 Optimal model selection using information criteria

The objective of the Akaike information criterion (AIC) is to compare the performance and complexity of models to select the optimal model while the Bayesian information criterion (BIC) applies a more significant penalty compared with the AIC (Eqs. (12 and 13)) [36]. The smallest value obtained by the AIC and/or BIC corresponds to the optimal model.

$$AIC = 2k - 2\ln(\hat{L}) \quad (12)$$

$$BIC = k\ln(n) - 2\ln(\hat{L}) \quad (13)$$

where \hat{L} is the maximum likelihood of the model, k is the number of parameters in the model, and n is the number of samples. The likelihood is a function of estimating the probability distribution y_n based on the data x_n with the specific weight θ of the model (i.e., how well the model describes the data when it has a specific weight (Eq. (14)). θ must be determined to ensure that the partial differentiation of the log-likelihood function for θ is zero. As a result, the maximum likelihood is estimated with the optimized θ (Eqs. (15 and 16)):

$$P(y|x, \theta) = \prod_{n=1}^N p(y_n|x_n, \theta) \quad (14)$$

$$\frac{\partial}{\partial \theta} \log P(y|x, \theta) = \sum_{n=1}^N \frac{\partial}{\partial \theta} \log p(y_n|x_n, \theta) = 0 \quad (15)$$

$$\theta_{MLE} = \operatorname{argmax}_{\theta} \sum_{n=1}^N \log p(y_n|x_n, \theta) \quad (16)$$

2.2.5 Diebold-Mariano test

The Diebold-Mariano (DM) test is a metric to compare the forecasting results. The null hypothesis of the DM test is that the forecasting result of the comparative model is consistent, and the closer the DM score is to 0, the more accurate the null hypothesis is established [37]. The DM-test has a negative value when the forecasting result of the first model is better than that of the second model. If the order of the models is reversed, the value of the DM-test can be positive.

$$\bar{d} = E[d_i] \quad (17)$$

$$e_i = y_i - f_i \quad (18)$$

$$r_i = y_i - g_i \quad (19)$$

$$\gamma_k = \frac{1}{n} \sum_{i=k+1}^n (d_i - \bar{d})(d_{i-k} - \bar{d}) \quad (20)$$

$$h = n^{1/3} + 1 \quad (21)$$

$$S_{DM} = \frac{\bar{d}}{\sqrt{[Y_0 + 2 \sum_{k=1}^{h-1} \gamma_k]/n}} \quad (22)$$

$$d_i = e_i^2 - r_i^2 \quad (23)$$

$$d_i = |e_i| - |r_i| \quad (24)$$

$$d_i = \left| \frac{e_i - y_i}{y_i} \right| \quad (25)$$

where e_i and r_i are the differences between the actual value y_i and predicted values f_i and g_i from the different models (Eqs. (18 and 19)), respectively, n is the number of forecast steps, γ_k is the covariance with k lags (Eq. (20)), and S_{DM} is the DM test score (Eq. (22)) that follows the standard Gaussian distribution if the null hypothesis is established. In the DM test, d_i is changed according to the selection of the loss function. When the loss function is the mean squared error (MSE), mean absolute deviation (MAD), and mean absolute percentage error (MAPE), d_i becomes Eq. (23), Eq. (24), and Eq. (25), respectively. A case study in this study employs the MSE.

2.2.6 Evaluation metrics

A set of R^2 score, root mean square error (RMSE), mean absolute error (MAE), and MAPE are applied for the developed framework as criteria for the evaluation of various forecasting models [38].

$$R^2 = 1 - \frac{\sum_{i=1}^n (y_i - \hat{y}_i)^2}{\sum_{i=1}^n (y_i - \bar{y}_i)^2} \quad (26)$$

$$RMSE = \sqrt{\frac{\sum_{i=1}^n (y_i - \hat{y}_i)^2}{n}} \quad (27)$$

$$MAE = \frac{1}{n} \sum_{i=1}^n |y_i - \hat{y}_i| \quad (28)$$

$$MAPE = \frac{100}{n} \sum_{i=1}^n \left| \frac{y_i - \hat{y}_i}{y_i} \right| \quad (29)$$

where y_i is the real value, \bar{y}_i is the mean value, and \hat{y}_i is the forecasting result. The closer the R^2 score is to 1, the better the model performance (Eq. (26)). It is recommended that other mode performance indicators are considered because difficulties in distinguishing biased models may arise [39]. The RMSE is the standard deviation of residuals based on the Euclidean distance between the real and predicted values (Eq. (27)). The MAE determines the accuracy of the model by calculating the arithmetic mean of the absolute error (Eq. (28)). The MAPE can avoid an underlying problem during data scaling but has several drawbacks (e.g., the denominator must always have non-zero values.) (Eq. (29)).

3. Results and Discussion

Figure 5 shows the SMP in a 3D heatmap from 2016 to 2021,

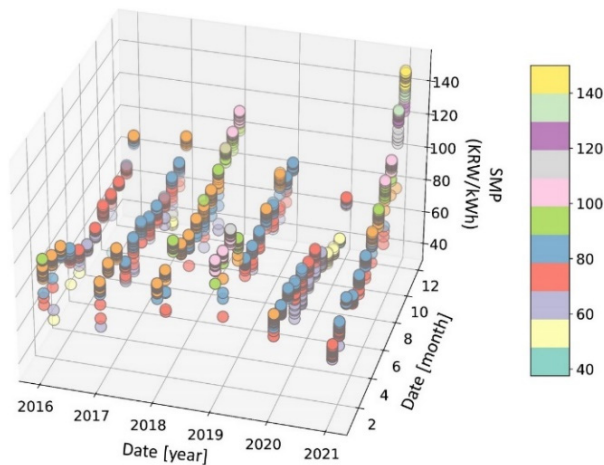


Figure 5. 3D heatmap of long-term historical data of SMP

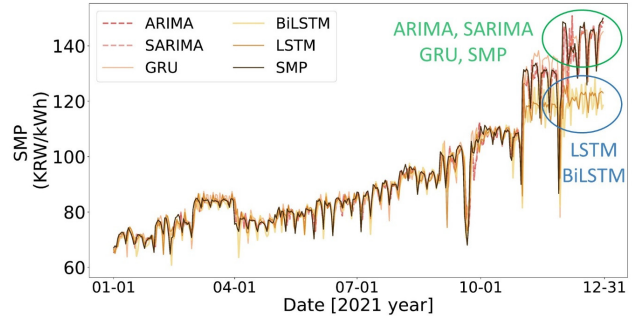


Figure 6. Test results of different forecasting models.

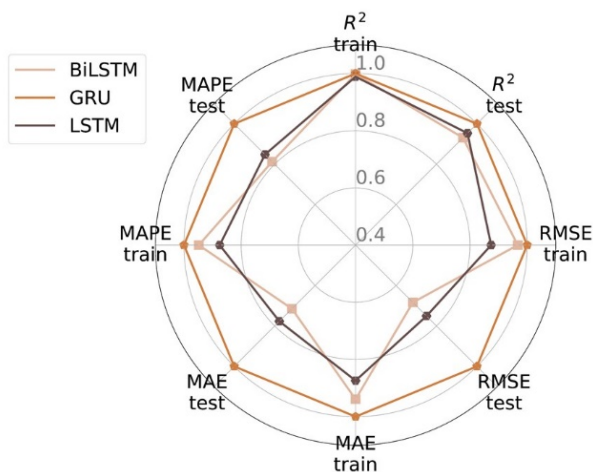
Table 3. Comparison of similarity between forecasting models using the DM test.

Set of models	MSE-based DM	p-value
SARIMA/ARIMA	0.68	0.518
BiLSTM/ARIMA	1.489	0.18
BiLSTM/SARIMA	1.472	0.185
GRU/ARIMA	0.743	0.482
GRU/SARIMA	0.558	0.594
GRU/BiLSTM	-1.407	0.202
LSTM/ARIMA	1.794	0.116
LSTM/SARIMA	1.784	0.118
LSTM/BiLSTM	2.307	0.054
LSTM/GRU	1.718	0.129

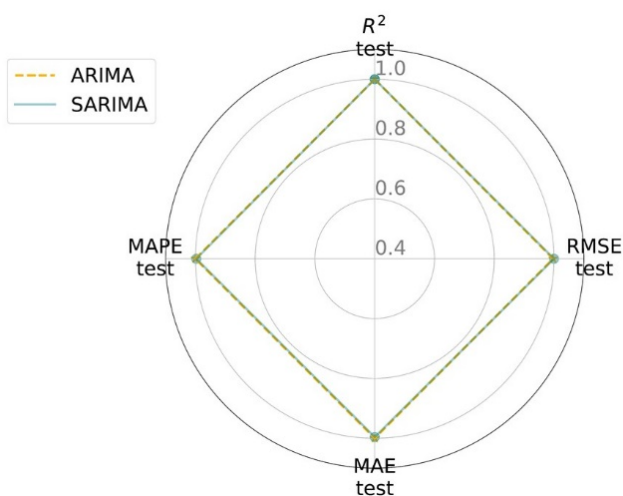
indicating that the SMP of 120 KRW/kWh or more is observed since November 2021. Thus, minimizing overfitting for training data is imperative to enhance the performance of the forecasting model. The suggested framework in this study not only considers the model performance score but also selects the optimal forecasting model using information criteria.

Figure 6 shows the results of various forecasting models. First, machine learning-based models, the ARIMA and SARIMA, learn the stationary data from trends and then begin to forecast. Then, it can be observed that the models are able to forecast rapidly rising patterns. In deep learning-based models, the LSTM and BiLSTM demonstrate good performance for a short-term forecast, whereas these models suffer when there is a rapidly rising pattern. However, the GRU performs well for both the long-term forecast and rapidly rising patterns.

Table 3 provides the comparison results of the forecast data for each model using a DM test. The model performance is analyzed with evaluation metrics, and model complexity is analyzed with the AIC/BIC model. The DM-test compares the forecasting results of the model. Therefore, DM-test was adopted to figure out an efficient model able to minimize computational costs and training time and maximize model performance. A set with the GRU and SARIMA shows the most similar DM score of 0.558, followed



(a) Radar chart of the deep learning-based models



(b) Radar chart of the machine learning-based models

Figure 7. Comparison of the forecasting models with a radar chart.

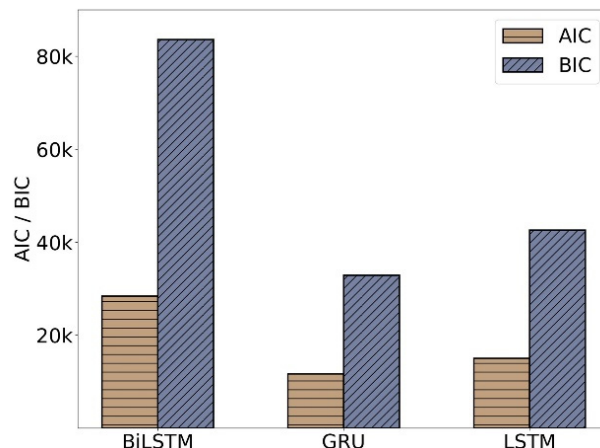
by the GRU/ARIMA and SARIMA/ARIMA with scores of 0.68 and 0.743, respectively. For the p-value of the other models, scores vary from 0.054 to 0.202, implying that the similarity of the results between any two models is less than 20%. It can be inferred that an optimal model selection should be conducted.

Table 4 shows the model performance for the evaluation metrics. In the training dataset, the GRU-based forecasting model outperforms other models (i.e., R^2 score: 0.965, RMSE: 2.489, MAE: 1.512, and MAPE: 0.02). In the test dataset, machine learning-based models and deep learning-based models are separately compared to reflect the approach of the algorithm structure (Figure 7). According to the results from the evaluation metrics, the ARIMA and SARIMA show similar performance. In the deep learning-based models, the GRU demonstrates great performance compared with the other deep learning-based forecasting models.

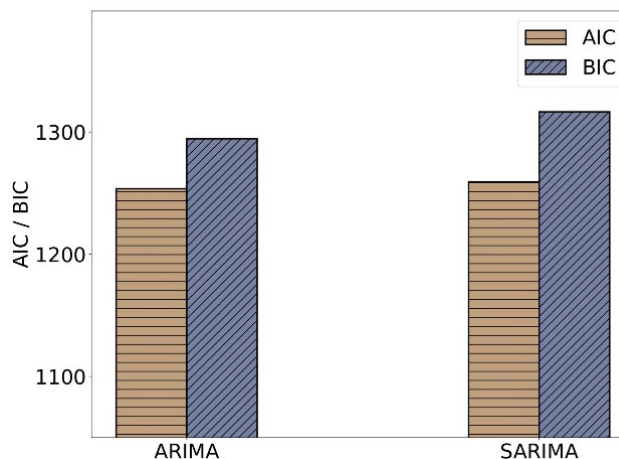
Finally, the AIC and BIC are used to compare the complexity of the models, and the optimal forecasting model is chosen. As previously mentioned, because deep learning-based models and

Table 4. Evaluation metrics for the forecasting models.

	BiLSTM	GRU	LSTM	ARIMA	SARIMA
Training dataset					
R^2	0.963	0.965	0.954	-	-
RMSE	2.574	2.489	2.848	-	-
MAE	1.61	1.512	1.73	-	-
MAPE	0.021	0.02	0.023	-	-
Test datasets					
R^2	0.878	0.943	0.899	0.972	0.972
RMSE	8.453	5.777	7.695	4.076	4.065
MAE	4.74	3.388	4.361	2.253	2.262
MAPE	0.048	0.039	0.046	0.025	0.025



(a) Bar chart of the AIC/BIC for the deep learning-based models



(b) Bar chart of the AIC/BIC for the machine learning-based models

Figure 8. Optimal forecasting models based on information criteria.

machine learning-based models rely on different algorithm structures, they have to be separately compared. For the deep learning-based models, the complexity of the GRU is the least with AIC and BIC scores of approximately 11,673 and 32,904, respectively. For the machine learning-based model, the ARIMA has the lowest AIC and BIC values corresponding to 1,253 and

1,294, respectively. Therefore, the results from the information criteria show that the ARIMA and GRU can be optimal forecasting models for the SMP.

As a future study, this work can be extended to develop hybrid models by combining diverse data-driven techniques such as wavelet transform and attention algorithms. Moreover, a significant data pipeline to better predict the SMP can be integrated with the proposed framework by considering implicit factors (e.g., oil prices, power plant costs, transportation and distribution system costs, and government regulations).

4. Conclusions

Research on SMP forecasting is crucial because inaccuracies in SMP forecasting can affect a variety of industries. In this study, the framework for SMP forecasting was developed and includes data processing, model development, model evaluation, and optimal model selection. A case study of South Korea was applied for the proposed framework using long-term time-series data from 2016 to 2021.

Machine learning-based models (ARIMA and SARIMA) and deep learning-based models (LSTM, BiLSTM, and GRU) were employed to construct the framework while the DM test and information criteria were integrated with traditional evaluation metrics. As a result, while the ARIMA and SARIMA demonstrated similar performance scores, in terms of information criteria, the optimal machine learning-based model was the ARIMA, showing AIC and BIC scores that were 0.45% and 1.67% lower than the SARIMA, respectively. In the case of the deep learning-based models, the GRU outperformed the other deep learning-based models (i.e., GRU demonstrated the highest R^2 score of 0.94, and the RMSE, MAE, and MAPE were approximately 31%, 28%, and 18% lower than the BiLSTM, which was identified as the worst model).

We believe that the proposed framework can be integrated with other algorithms and data variables to contribute to SMP-related research and the electricity energy market.

Acknowledgement

This work was supported by the projects NRF-2021R1F1A1 059919 and NRF-2020M1A2A2080858 through the National Research Foundation of Korea (NRF) and the Ministry of Science, ICT & Future Planning.

References

1. Sepulveda, C.F., "Explaining the demand and supply model with the cost-benefit rule," *Int. Rev. Econ., Educ.*, **35**(8), 100194

(2020).

2. Takemura, R., "Economic reasoning with demand and supply graphs," *Math. Soc. Sci.*, **103**, 25-35 (2020).
3. Djørup, S., Thellufsen, J.Z., and Sorknæs, P., "The electricity market in a renewable energy system," *Energy*, **162**, 148-157 (2018).
4. Barroso, L.A., Cavalcanti, T.H., Giesbertz, P., and Purchala, K., "Classification of electricity market models worldwide," *2005 CIGRE/IEEE PES International Symposium*, (i), 9-16 (2005).
5. Moreno, B., and Díaz, G., "The impact of virtual power plant technology composition on wholesale electricity prices: A comparative study of some European Union electricity markets," *Renew. Sustain. Energy Rev.*, **99**(4), 100-108 (2019).
6. Sahriatzadeh, F., Nirbhavane, P., and Srivastava, A.K., "Locational marginal price for distribution system considering demand response," *2012 North American Power Symposium, NAPS 2012*, 1-5 (2012).
7. Murshed, M., and Tanha, M.M., "Oil price shocks and renewable energy transition: Empirical evidence from net oil-importing South Asian economies," *Energy, Ecology Environ.*, **6**(3), 183-203 (2021).
8. Borovkova, S., and Schmeck, M.D., "Electricity price modeling with stochastic time change," *Energy Econ.*, **63**, 51-65 (2017).
9. Yu, S., Fang, F., Liu, Y., and Liu, J., "Uncertainties of virtual power plant: Problems and countermeasures," *Appl. Energy*, **239** (1), 454-470 (2019).
10. Taner, T., "Economic analysis of a wind power plant: A case study for the Cappadocia region," *J. Mechani Sci. Technol.*, **32**(3), 1379-1389 (2018).
11. Arcos-Vargas, A., Cansino, J.M., and Román-Collado, R., "Economic and environmental analysis of a residential PV system: A profitable contribution to the Paris agreement," *Renew. Sustain. Energy Rev.*, **94** (6), 1024-1035 (2018).
12. Rincon, L., Puri, M., Kojakovic, A., and Maltsoğlu, I., "The contribution of sustainable bioenergy to renewable electricity generation in Turkey: Evidence based policy from an integrated energy and agriculture approach," *Energy Policy*, **130**(3), 69-88 (2019).
13. Byers, E.A., Coxon, G., Freer, J., and Hall, J.W., "Drought and climate change impacts on cooling water shortages and electricity prices in Great Britain," *Nature Commun.*, **11**(1), 1-12 (2020).
14. Fan, J.L., Hu, J.W., and Zhang, X., "Impacts of climate change on electricity demand in China: An empirical estimation based on panel data," *Energy*, **170**, 880-888 (2019).
15. Zheng, S., Huang, G., Zhou, X., and Zhu, X., "Climate-change impacts on electricity demands at a metropolitan scale: A case study of Guangzhou, China," *Appl. Energy*, **261**(12), 114295 (2020).
16. Tsai, C.H., and Tsai, Y.L., "Competitive retail electricity market under continuous price regulation," *Energy Policy*, **114**(2),

- 274-287 (2018).
17. Ciarreta, A., Pizarro-Irizar, C., and Zarraga, A., "Renewable energy regulation and structural breaks: An empirical analysis of Spanish electricity price volatility," *Energy Econ.*, **88**, 104749 (2020).
 18. Kuo, P.H., and Huang, C.J., "An electricity price forecasting model by hybrid structured deep neural networks," *Sustainability (Switzerland)*, **10**(4), 1-17 (2018).
 19. Sarwar, S., Chen, W., and Waheed, R., "Electricity consumption, oil price and economic growth: Global perspective," *Renew. Sustain. Energy Rev.*, **76**(6), 9-18 (2017).
 20. Jung, S., Kim, H., and Won, D., "A Study on the Effect of SMP Volatility on Power Supply in Korea," *J. Ind. Econ. Bus.*, **31**(3), 1057-1077 (2018).
 21. Review, R.E., "A Study on the Effects of the System Marginal Price Setting Mechanism of the Cost Function in Operating Modes of the Combined Cycle Power Plants in Korea Electricity Market," *Environ. Resour. Econ. Rev.*, **30**(1), 107-128 (2021).
 22. Aggarwal, S.K., Saini, L.M., and Kumar, A., "Electricity price forecasting in deregulated markets: A review and evaluation," *Int. J. Electr. Power Energy Sys.*, **31**(1), 13-22 (2009).
 23. Weron, R., "Electricity price forecasting: A review of the state-of-the-art with a look into the future," *Int. J. Forecast.*, **30**(4), 1030-1081 (2014).
 24. Shyu, M., Chen, S., and Iyengar, S.S., "A Survey on Deep Learning: Algorithms , Techniques ," *ACM Comput. Surv.*, **51**(5), 1-36 (2018).
 25. Li, S., Li, W., Cook, C., Zhu, C., and Gao, Y., "Independently recurrent neural network (indrnn): Building a longer and deeper rnn," *Proceedings of the IEEE conference on computer vision and pattern recognition*, 5457-5466 (2018).
 26. Le, X.H., Ho, H.V., Lee, G., and Jung, S., "Application of Long Short-Term Memory (LSTM) neural network for flood forecasting," *Water (Switzerland)*, **11**(7), (2019).
 27. Dey, R., and Salem, F.M., "Gate-variants of Gated Recurrent Unit (GRU) neural networks," *2017 IEEE 60th International Midwest Symposium on Circuits and Systems (MWSCAS)*, 1597-1600 (2017).
 28. Wang, S., Wang, X., Wang, S., and Wang, D., "Bi-directional long short-term memory method based on attention mechanism and rolling update for short-term load forecasting," *International J. Electri. Power Energy Sys.*, **109** (1), 470-479 (2019).
 29. Nam, K.J., Hwangbo, S., and Yoo, C.K., "A deep learning-based forecasting model for renewable energy scenarios to guide sustainable energy policy: A case study of Korea," *Renew. Sustain. Energy Rev.*, **122** (12), 109725 (2020).
 30. Chang, Z., Zhang, Y., and Chen, W., "Electricity price prediction based on hybrid model of adam optimized LSTM neural network and wavelet transform," *Energy*, **187**, 115804 (2019).
 31. Qiao, W., and Yang, Z., "Forecast the electricity price of U.S. using a wavelet transform-based hybrid model," *Energy*, **193**, 116704 (2020).
 32. Makridakis, S., Spiliotis, E., and Assimakopoulos, V., "Statistical and Machine Learning forecasting methods: Concerns and ways forward," *PLoS ONE*, **13**(3), (2018).
 33. Wu, D.C.W., Ji, L., He, K., and Tso, K.F.G., "Forecasting Tourist Daily Arrivals With A Hybrid Sarima-Lstm Approach," *J. Hospitality Tourism Res.*, **45**(1), 52-67 (2021).
 34. Dimri, T., Ahmad, S., and Sharif, M., "Time series analysis of climate variables using seasonal ARIMA approach," *J. Earth Sys. Sci.*, **129**(1), (2020).
 35. Qi, H., Xiao, S., Shi, R., Ward, M.O., Chen, Y., Tu, W., Su, Q., Wang, W., Wang, X., and Zhang, Z., "Hyper-Parameter Optimization: A Review of Algorithms and Applications," *Nature*, **388**, 539-547 (2018).
 36. Mendyk, A., Jachowicz, R., Fijorek, K., Dorozyński, P., Kulinowski, P., and Polak, S., "KinetDS: An open source software for dissolution test data analysis," *Dissolut. Technol.*, **19**(1), 6-11 (2012).
 37. Zhang, Y., Ma, F., and Wei, Y., "Out-of-sample prediction of the oil futures market volatility: A comparison of new and traditional combination approaches," *Energy Econ.*, **81**(8), 1109-1120 (2019).
 38. Handelman, G.S., Kok, H.K., Chandra, R. V, Razavi, A.H., Huang, S., Brooks, M., Lee, M.J., and Asadi, H., "Peering into the black box of artificial intelligence: evaluation metrics of machine learning methods," *Am. J. Roentgenol.*, **212**(1), 38-43 (2019).
 39. Rustam, F., Reshi, A.A., Mehmood, A., Ullah, S., On, B.-W., Aslam, W., and Choi, G.S., "COVID-19 future forecasting using supervised machine learning models," *IEEE access*, **8**, 101489-101499 (2020).